

ELECTRON MICROSCOPY INSPIRED SETUP FOR SINGLE-SHOT 4-D TRACE SPACE RECONSTRUCTION OF BRIGHT ELECTRON BEAMS*

J. Giner Navarro[†], D. Cesar, P. Musumeci, UCLA, 90095 Los Angeles, USA
 R. Assmann, B. Marchetti, D. Marx¹, DESY, 22607 Hamburg, Germany
¹also at Universitat Hamburg, Hamburg, Germany

Abstract

In the development of low charge, single-shot diagnostics for high brightness electron beams, Transmission Electron Microscopy (TEM) grids present certain advantages compared to pepper pot masks due to higher beam transmission. In this paper, we developed a set of criteria to optimize the resolution of a point projection image. However, this configuration of the beam with respect to the grid and detector positions implies the measurement of a strongly correlated phase space which entails a large sensitivity to small measurement errors in retrieving the projected emittance. We discuss the possibility of an alternative scheme by inserting a magnetic focusing system in between the grid and the detector, similar to an electron microscope design, to reconstruct the phase space when the beam is focused on the grid.

INTRODUCTION

The development of ultra-low emittance diagnostics is instrumental for validating predictive models to efficiently push the limits of high brightness electron beams [1]. There is special interest in measuring the core brightness since it is an important parameter characterizing rf photoinjector sources [2]. Emittance measurements with the well-known pepper pot technique [3] allow us to reconstruct the beam transverse phase space from a single shot, in contrast to other standard multi-shot methods such as the solenoid or quadrupole scan. TEM grids with thin, perpendicular bars have also been tested to measure emittance [4] and have been proven to be an interesting alternative for single-shot diagnostics when used in very low charge (sub-pC) beam experiments such as ultrafast electron diffraction [5], since they offer larger beam transmission than pepper pot masks.

In this paper we discuss the requirements of the beam optics and grid dimensions to efficiently perform emittance measurements with TEM grids, as they present more stringent constraints to optimize the visibility of the thin bars. A variation of this technique is also suggested by inserting a focusing lens in between the mask and the detector which promises to allow measurements of sub-nm geometric emittances.

TEM GRID TECHNIQUE

The reconstruction of 4-D transverse trace space using TEM grids is analogous to the pepper pot technique. The

* This work has been partially supported by the National Science Foundation under Grant No. 1549132 and Department of Energy under award No. DE-SC0009914.

[†] jorge.giner.navarro@gmail.com

beam is masked with the grid and a point projection image is obtained at the detector downstream (see Fig. 1). The result is a magnified image of the beam profile sampled by the shadow of grid bars.

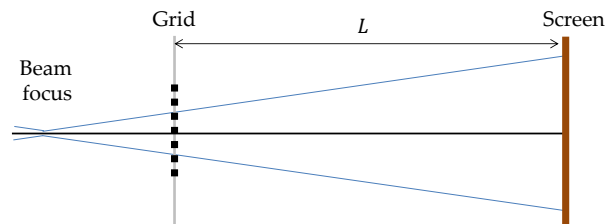


Figure 1: Scheme of emittance measurement setup using TEM grids.

For the measurement of the horizontal emittance, an image processing routine has been developed to analyze the intensity profile across each single vertical bar that divides two adjacent beamlets. The following fitting function [4] is used to retrieve the average and rms angle, \bar{x}'_i and $\sigma_{x',i}$, and the density of particles, I_i , intercepted by the bar under analysis (denoted by subscript i):

$$f_i(X) = I_i + P_{1,i}(X - \bar{X}_i) + P_{2,i} \left[\operatorname{erf} \left(\frac{(X - \bar{X}_i) - M_x a/2}{\sqrt{2}\sigma_{X,i}} \right) - \operatorname{erf} \left(\frac{(X - \bar{X}_i) + M_x a/2}{\sqrt{2}\sigma_{X,i}} \right) \right]$$

where a is the bar width, M_x is the magnification of the grid image, L is the drift length between the grid and the detector, and the fitting parameters are: I_i is the charge intercepted by the bar, $\bar{X}_i = x_i + L\bar{x}'_i$ is the center position of the bar at the detector (where x_i is the center position at the grid), $\sigma_{X,i} = L\sigma_{x',i}$ is the rms spread of the intercepted particles, and $P_{1,i}, P_{2,i}$ take into account a linear variation of charge density along the direction that crosses the bar. The grid bars position x_i and the fitted parameters $\{\bar{x}'_i, \sigma_{x',i}, I_i\}$ are applicable into the standard pepper pot formulas [3] to retrieve the beam matrix elements, $\langle x^2 \rangle$, $\langle xx' \rangle$ and $\langle x'^2 \rangle$, for the evaluation of the 2D projected emittances:

$$\epsilon_x = \sqrt{\langle x^2 \rangle \langle x'^2 \rangle - \langle xx' \rangle^2} \quad (1)$$

The same analysis is valid for the vertical emittance by processing the shadow of the horizontal bars. The interpolation of the fitted parameters to the bar intersections allows the computation of the beam matrix coupling terms and the 4-D rms emittance.

Furthermore, as the beam phase space is sampled in multiple points by the grid bars, it is possible to reconstruct the

full 4-D trace space density by the superposition of the different beamlets. Hence, the core brightness and core emittance can be retrieved by analyzing the reconstructed density of particles at the core of the trace space [6].

The success of the analysis strongly depends on the quality of the image used to identify the grid bars covered by the beam transverse profile. Three important requirements concerning the beam optics and the experimental setup must be satisfied:

1. The beam needs to be transversely intercepted by a sufficient number of bars of the TEM grid to minimize sampling errors. The choice of the grid mesh size determines a lower limit of the beam size that can be profiled:

$$\sqrt{\langle x^2 \rangle} \gg d \quad (2)$$

where d is the grid spacing and $\langle x^2 \rangle$ corresponds to the transverse beam matrix element at the grid plane. TEM grids are commercially available with different mesh sizes, from a rough mesh of few hundreds of μm to ultrafine mesh of $10 \mu\text{m}$.

2. As the beam propagates after the grid, the angular divergence of each beamlet $\sigma_{x'}$ causes blurring of the bar edges. A possible overlap of two adjacent beamlets due to this blurring effect would compromise the localization of the bar at the detector, thus the following inequality must be satisfied:

$$M_x \frac{a}{2} \gg L \sigma_{x',i} \quad (3)$$

where M_x is the magnification factor and is given by:

$$M_x = 1 + L \frac{\langle xx' \rangle}{\langle x^2 \rangle} \quad (4)$$

and $\langle xx' \rangle$, $\langle x^2 \rangle$ are the second moments of the beam at the grid plane.

3. At the same time, the detector must be capable of resolving the shadow profile in order to retrieve the angular divergence $\sigma_{x'}$ of the particles blocked by the bar. Assuming that the resolution of the detector is limited by the point-spread function, σ_{PSF} , of the screen:

$$L \sigma_{x',i} \gg \sigma_{\text{PSF}} \quad (5)$$

Considering a reasonable distance L that assures enough resolution (Eq. (5)), the magnification must be increased by separating the beam waist from the grid to maximize the $\langle xx' \rangle$ and satisfy Eq. (3). Maximizing $\langle xx' \rangle$ implies a strongly correlated ellipse in the $x-x'$ subspace at the grid plane, such that the geometric emittance (see Eq. (1)) turns out to be a subtraction of two similar large numbers. Thus, although this technique is effective to reconstruct the transverse beam matrix, this configuration is not favorable for the evaluation of ultra low geometric emittances as it is extremely sensitive to small errors of the matrix elements. A new experimental scheme is proposed in the following section to measure the emittance from a more convenient phase space geometry.

THE GRID-LENS SCHEME

Moving the beam focus closer to the grid makes $\langle xx' \rangle$ smaller and diminishes the sensitivity of small geometric emittances. However, the magnification drops when reducing $\langle xx' \rangle$ according to Eq. (4). Inserting a beam-focusing lens between the grid and the screen increases the magnification while having less $x-x'$ correlation at the grid plane. Assuming an uncoupled beam transport from the grid to the screen, defined by the matrix R , the magnification of the grid dimensions is given by:

$$M_x = R_{11} + R_{12} \frac{\langle xx' \rangle}{\langle x^2 \rangle} \quad (6)$$

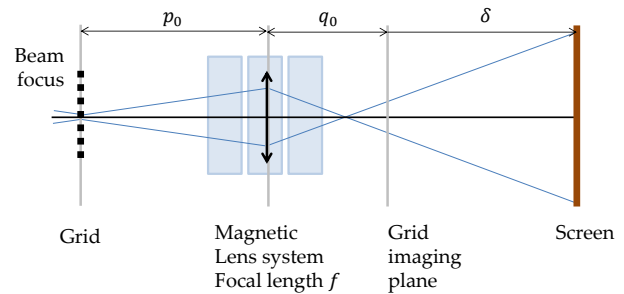


Figure 2: Grid-lens scheme for emittance measurement setup using a magnetic focusing system.

The proposed grid-lens scheme is shown in Fig. 2. The formalism of the trace space reconstruction is analogous to the standard grid technique, with the exception of obtaining an inverted image of the bar positions due to the lens effect (negative magnification). The evaluation of the average and rms angle of the particles intercepted by the bar is:

$$\bar{x}'_i = \frac{\bar{X}_i - R_{11} x_i}{R_{12}} \quad (7)$$

$$\sigma_{x'} = \frac{\sigma_X}{|R_{12}|} \quad (8)$$

The elements R_{12} and R_{34} play the same role as the drift length in the standard method and the elements R_{11} and R_{33} are the horizontal and vertical magnification factors, M_x and M_y , respectively, when the beam is focused on the grid.

When the screen is positioned at the image plane of the object, the elements R_{12} and R_{34} are very small. In this case, the screen shows an image of the grid with sharp, in-focus bar edges. This condition is not applicable to the beam phase space measurement because it does not provide any information of the angular distribution (see Eqs. (7) and (8)). For this reason, an additional defocus needs to be adjusted by moving the screen off of the imaging plane or varying the focal strength of the magnetic lens.

The requirements of the resulting beam profile at the detector are the same as the ones applied to the standard grid technique in the previous section. Given the finite spatial resolution of the screen, there must be sufficient defocus of

the bar edges to allow for the analysis of the angular divergence of the intercepted particles. At the same time, this defocus must be limited by the separation of adjacent beamlets in order to avoid overlapping. Equations (3) and (5) are reformulated as:

$$|R_{11}| \frac{a}{2} \gg |R_{12}| \sigma_{x'} \quad (9)$$

$$|R_{12}| \sigma_{x'} \gg \sigma_{\text{PSF}} \quad (10)$$

With regards to the beam-focusing system, a magnetic quadrupole triplet offers good control of the beam size magnification in order to optimize the measurements at the detector. In addition, the system offers flexibility in adjusting horizontal and vertical magnification factors for emittance measurements in flat beams, which can be tailored to accomplish ultra-low emittance in one of the planes for interesting applications, such as dielectric laser accelerators [7]. An accurate characterization of the transport optics is crucial in the beam phase space reconstruction. An off-line calibration of the relevant transport matrix elements, i.e. R_{11} , R_{12} , R_{33} and R_{34} , can be made by scanning the entry position and angle of the beam into the focusing lens with steering magnets and measuring the response position at the detector downstream.

Given the gain in magnification offered by the lens, the measurement of very small beam sizes is accessible with ultra fine mesh grids. The proposed diagnostic scheme becomes a powerful tool for measuring ultra-low geometric emittances by sampling beams with very small waists and angular divergence. This experimental setup shares some specifications and requirements with high-brightness electron beam microscope experiments [8,9]. The grid-lens scheme meets similar challenges such as aberration of strong magnetic quadrupoles, beam dynamics limited by tight apertures of the magnets and space-charge effects that would compromise the validity of the linear transport matrix formulation. The experience in the performance optimization of strong focusing systems for low-emittance beams could be transferred to the development of sub-nm geometric emittance diagnostics.

The application of the single-shot 4-D trace space reconstruction in the grid-lens technique has been tested in simulations with ultra-low emittance beams. The (x, x', y, y') coordinates of one million particles have been generated in MATLAB following an uncorrelated Gaussian distribution with a round beam profile of $30 \mu\text{m}$ rms size and 0.5 nm rad geometric emittance. A TEM2000 grid mask ($12.7 \mu\text{m}$ pitch and $7.5 \mu\text{m}$ bar width) has been introduced to exclude the particles that are intercepted by the bars. The beam has been propagated to the grid using the transfer matrix of a stigmatic focusing system, with a total focal length 3 cm . No space-charge has been considered in the propagation. The location of the lens has been optimized, according to Eqs. (9) and (10), to obtain a satisfactory image of the beam which allows the characterization of the trace space. The lens is positioned 16 cm after the grid such that we obtain a magnification of $M_x = M_y = -22$ with a defocus length

(that is the distance between the screen and the grid image plane) of 65 cm . A realistic pixel binning of the detector at pitch of $15 \mu\text{m}$ and a finite point spread function of $30 \mu\text{m}$ have been also taken into account in the simulation. The resulting image is shown in Fig. 3. The results of the emittance reconstruction algorithm are summarized in Table 1 and show good agreement with the simulation parameters.

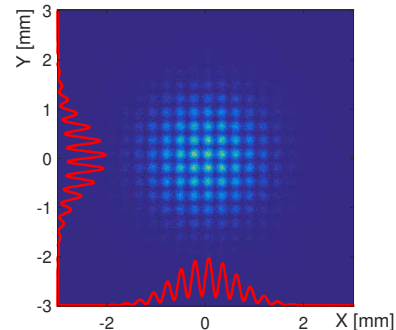


Figure 3: Profile of simulated electron beam of 0.5 nm rad geometric emittance sampled with a TEM2000 grid.

Table 1: Reconstructed emittance from the simulation of a grid-lens diagnostic setup tested with a 0.5 nm rad beam.

[nm rad]	Original	Reconstruction
ϵ_x	0.500	0.520
ϵ_y	0.500	0.514
$\epsilon_{\text{core},x}$	0.250	0.189
$\epsilon_{\text{core},y}$	0.250	0.157
$\sqrt{\epsilon^{4D}}$	0.500	0.517
$\sqrt{\epsilon_{\text{core}}^{4D}}$	0.236	0.286

CONCLUSIONS

The performance of the single-shot 4-D trace space diagnostics using TEM grids is very sensitive to the beam optics and the grid dimensions. We have formulated a set of criteria to assess the quality of the resulting image at the detector for the phase space reconstruction algorithm. These equations show that the best configuration is a point projection of the grid, which is subject to significant errors in retrieving the emittance. A grid-lens scheme allows us to measure a less correlated $x-x'$ distribution by increasing the magnification. Simulations show that an analogous analysis applied to this scheme can be used to reconstruct the phase space of smaller emittance beams even at a tight focus. There are plans for a future dedicated experiment to apply the new trace space reconstruction scheme on UCLA's Pegasus ultrafast electron beamline, which will benefit from the hardware and experience of an ongoing microscope experiment [10].

REFERENCES

- [1] P. Musumeci *et al.*, “Advances in Bright Electron Sources”, *Nuclear Instruments and Methods in Physics Research A*, to be published.
- [2] I. V. Bazarov *et al.*, “Maximum Achievable Beam Brightness from Photoinjectors” *Phys. Rev. Lett.*, vol. 102, p. 104801, 2009.
- [3] M. Zhang, “Emittance formula for slits and pepper-pot measurement”, Fermilab, IL, USA, Rep. Fermilab-TM-1998, 1996.
- [4] R. K. Li *et al.*, “Nanometer emittance ultralow charge beams from rf photoinjectors” *Phys. Rev. ST Accel. Beams* vol. 15, p. 090702, 2012.
- [5] X. J. Wang *et al.*, “Femto-second electron beam diffraction using photocathode rf gun”, in *Proc. 2003 Particle Accelerator Conference (IPAC'03)*, paper WOAC003, 2003.
- [6] I. V. Bazarov *et al.*, “Benchmarking of 3D space charge codes using direct phase space measurements from photoemission high voltage dc gun”, *Phys. Rev. ST Accel. Beams*, vol. 11, p. 100703, 2008.
- [7] A. Ody *et al.*, “Flat electron beam sources for DLA accelerators”, *Nuclear Instruments and Methods in Physics Research A*, vol. 865 pp. 75–83, 2017.
- [8] C. Lu *et al.*, “Imaging nanoscale spatial modulation of a relativistic electron beam with a MeV ultrafast electron microscope”, *Appl. Phys. Lett.*, vol. 112, p. 113102, 2018.
- [9] R. K. Li and P. Musumeci, “Single-Shot MeV Transmission Electron Microscopy with Picosecond Temporal Resolution”, *Phys. Rev. Applied*, vol. 2, p. 024003, 2014.
- [10] D. Cesar *et al.*, “Demonstration of Single-Shot Picosecond Time-Resolved MeV Electron Imaging Using a Compact Permanent Magnet Quadrupole Based Lens”, *Phys. Rev. Lett.*, vol. 117, p. 024801, 2016.